Acute Respiratory Distress Syndrome is a TH17 and Treg immune disease

By Wan-Jiung Hu
Postdoctorate
Genomics Research Center
Academia Sinica
No 128 Academia Road section2
Nangang 115, Taipei, Taiwan

Previous Institutes:

Department of Pediatrics
Taipei Municipal Chung-Hsin Hospital

Department of Internal Medicine
Taipei Tzu-Chi Buddhist Hospital (Medical Center)

Department of Neurology
Taipei Mackay Memorial Hospital (Medical Center)

Graduate Institute of Immunology
National Taiwan University College of Medicine

Department of International Health (Vaccine science track)
Johns Hopkins University Bloomberg School of Public Health

Abstract

Acute Respiratory Distress Syndrome (ARDS) is a very severe syndrome leading to respiratory failure and subsequent mortality. Sepsis is the leading cause of acute respiratory distress syndrome. Thus, extracellular bacteria play an important role in the pathophysiology of ARDS. Overactivated neutrophils are the major effector cells in ARDS. Thus, extracellular bacteria triggered TH17 host immunity with neutrophil activation counts for the etiology of ARDS. Here, I use microarray analysis to describe TH17 related cytokine up-regulation in whole blood of ARDS patients. In addition, TGF-β secreting Treg cells play important roles in lung fibrosis. Thus, ARDS is actually a TH17 and Treg immune disorder.

About the author

Wan-Jiung Hu is a MD PhD. His former name is Wan-Chung Hu. His MD degree was awarded from National Taiwan University. His PhD degree was awarded from Vaccine science track of Department of International Health of Johns Hopkins University. His PhD thesis was using microarray to identify the host immunological pathway after malaria infection. His first first-author paper: “Common and divergent immune response signaling pathways discovered in peripheral blood mononuclear cell gene expression patterns in presymptomatic and clinically apparent malaria” is published in Infection and Immunity in 2006 October. Thus, he first proposed the THαβ immunity which is host immunity against viruses. A subsequent paper in 2008 called it TH9 immunity. However, TH9 immunity is not a good name since IL-9 is a TH2 cytokine. He was trained as a neurology resident in Department of Neurology of Taipei Mackay Memorial Hospital of Taiwan. Currently, he is doing postdoc research in Genomic Research Center of Academia Sinica, Taiwan. His current research topic is cancer immunotherapy. Besides, he is doing functional genomics studies. The author would like to publish this manuscript. If journal editors are interested in this paper, please feel free to contact me. While I am preparing this manuscript, I find that my computer has abnormal activity. I think certain hacker is invading my computer. Thus, I need to post this manuscript ASAP onto Vixra in order to prevent the hacker to steal this content. Most of all, the discussion part is most important. I need to fight against the hacker until he loses everything.

Introduction

Acute respiratory distress syndrome (ARDS) is a severe cause of respiratory failure. Despite of current treatment, the mortality rate is very high. We still don’t have successful management strategies to deal with ARDS. Most important of all, we still don’t know the exact pathophysiology of ARDS. Sepsis or bacteremia is the leading cause of ARDS. Besides, neutrophil activation is reported in many studies of lung of ARDS patients. Thus, extracellular bacteria induced TH17 immunity overactivation should be the etiology of ARDS. Here, I use a microarray analysis to study immune-related gene profiles in peripheral leukocytes of ARDS patients. I found several TH17 related effector molecules are activated in ARDS. That supports that ARDS is a TH17 dominant inflammatory disease.

Material and Methods

Microarray dataset

According to Dr. J. A. Howrylak's research in Physiol Genomics 2009, he collected total RNA from whole blood in sepsis and ARDS patients. He tried to find out molecular signature of ARDS compared to sepsis patients. His dataset is available in Gene Expression Omnibus (GEO) www.ncbi.nlm.nih.gov/geo (assession number GSE 10474). The second dataset is from GSE20189 of Gene Expression Omnibus. This dataset was collected by Dr. Melissa Rotunno in Cancer Prevention Research 2011. Molecular signature of early stage of lung adenocarcinoma was studied by microarray. I use the healthy control whole blood RNA from this dataset to compare the ARDS patients. In this study, I perform further analysis to study peripheral leukocyte gene expression profiles of ARDS compared to those of healthy controls.

Statistical analysis

Affymetrix HG-U133A 2.0 genechip was used in both samples. RMA express software(UC Berkeley, Board Institute) is used to do normalization and to rule out the outliners of the above dataset. I rule out the potential outliners of samples due to the following criteria:

1. Remove samples which have strong deviation in NUSE plot
2. Remove samples which have broad spectrum in RLE value plot
3. Remove samples which have strong deviation in RLE-NUSE mutiplot
4. Remove samples which exceed 99% line in RLE-NUSE T2 plot

RT-PCR confirmation

Dr. J. A. Howrylak performed real time PCR for selected transcripts (cip1, kip2) by using TaqMan Gene Expression Assays (Applied Biosystems, Foster City, CA). In the second dataset, Dr. Melissa Rotunno also performed qRT-PCR test to validate the microarray results. RNA quantity and quality was determined by using RNA 600 LabChip-Aligent 2100 Bioanalyzer. RNA purification was done by the reagents from Qiagen Inc. All real-time PCRs were conducted by using an ABI Prism 7000 Sequence Detection System with the designed primers and probes for target genes and an internal control gene-GAPDH. This confirms that their microarray results are convincing compared to RT-PCR results.

Results

RMA analysis of whole blood from healthy normal control

The RMA analysis was performed for RNA samples from whole blood of healthy control of the lung adenocarcinoma dataset. Raw boxplot, NUSE plot, RLE value plot, RLE-NUSE multiplot, and RLE-NUSE T2 plot were generated. Then, sample was included and excluded by using these graphs(Figure 1A, 1B, 1C, 1D, 1E)

RMA analysis of whole blood from acute lung injury patients

The RMA analysis was performed for RNA samples from whole blood of healthy control of the ARDS dataset. Raw boxplot, NUSE plot, RLE value plot, RLE-NUSE multiplot, and RLE-NUSE T2 plot were generated. Then, sample was included and excluded by using these graphs(Figure 2A, 2B, 2C, 2D, 2E)

TH17 and Treg related genes are up-regulated in ARDS

Based on the microarray analysis, I find out that many TH17 related genes are up-regulated in ARDS including Toll-like receptors 1,2,4,5,8, complement, heat shock protein 70, cathpesin, S100A proteins, leukotrienes, defensins, TH17 chemokines, and MMPs. Many fibrosis related genes are also up-regulated including key collagen synthesis enzymes and fibroblast growth factor. Key TH17 initiating cytokines including TGF beta and IL-6 are also up-regulated. This explains that TH17 immunity is initiated in ARDS. NK cell and T cell related genes are down-regulated. This explains that TH1 or THαβ immunological pathway is not triggered in ARDS. (Table 1-14)

Discussion

Acute respiratory distress syndrome (ARDS) is a very severe respiratory complication. Sepsis is the major risk factor of ARDS. Sepsis is the uncontrolled bacteremia by extracellular bacteria infection. In addition, PMNs overactivation is very important in the pathogenesis of ARDS. Thus, extracellular bacteria induced TH17 immunity with neutrophil activation should be the key in the pathophysiology of ARDS.

According to Harrison's internal medicine, the time course of ARDS can be divided into three stages. First, the exudative phase. In this phase, injured alveolar capillary endothelium and type I pneumocytes cause the loss of tight alveolar barrier. Thus, edema fluid rich in protein accumulate in the interstitial alveolar spaces. It has been reported that cytokines (IL-1, IL-6, and TNF-α) and chemokines (IL-8, and leukotriene

B4) are present in lung in this phase. A great numbers of neutrophils traffic into the pulmonary interstitium and alveoli. Alveolar edema predominantly leads to diminished aeration and atelectasis. Hyaline membranes start to develop. Then, intrapulmonary shunting and hypoxemia develop. The situation is even worse with microvascular occlusion which leads to increasing dead space and pulmonary hypertension. The exudative phase encompasses the first seven days of disease after exposure to a precipitating ARDS risk factor such as sepsis, aspiration pneumonia, bacteria pneumonia, pulmonary contusion, near drowning, toxic inhalation injury, severe trauma, burns, multiple transfusions, drug overdose, pancreatitis, and post-cardiopulmonary bypass.

Second, proliferative phase. This phase usually lasts from day 7 to day 21. Although many patients could recover during this stage, some patients develop progressive lung injury and early change of pulmonary fibrosis. Histologically, this phase is the initiation of lung repair, organization of alveolar exudates, and a shift from a neutrophil to a lymphocyte dominant pulmonary infiltrate. There is a proliferation of type II pneumocytes which can synthesize new pulmonary surfactants. They can also differentiate into type I pneumocytes. In addition, there is beginning of type III procollagen peptide presence which is the marker of pulmonary fibrosis.

Third, fibrotic phase. Although many patients with ARDS recover lung function three weeks after the initial lung injury, some enter a fibrotic phase that may require long term support on mechanical ventilators. Histologically, the alveolar edema and inflammatory exudates in early phases are converted to extensive alveolar duct and interstitial fibrosis. Intimal fibroproliferation in the pulmonary microvascular system leads to progressive vascular occlusion and pulmonary hypertension.

Here, I propose a detail pathogenesis to explain the three stages of ARDS. In the first exudative stage, neutrophils are attracted to lung due to chemotaxic agents such as IL-8. During sepsis, bacterial infection in pulmonary tissue can trigger pulmonary epithelial cells, pulmonary endothelial cells, pulmonary fibroblast, and alveolar macrophage to be activated. Toll-like receptors 1,2,4,5 as well as heat shock proteins (HSP60, HSP70,HSP90) are key molecules to trigger TH17 host immunity. Heat sock proteins are important stress proteins in situation such as burn, trauma, hemorrhagic shock, near drowning or acute pancreatitis. Thus, TH17 related cytokines such as IL-17, IL-1, TNF-α, and IL-6 as well as TH-17 related chemokines such as IL-8 and other CXCL group chemokines will be triggered. TH17 cytokines will start to activate TH17 immunity including activating PMN effector function and drive T helper cells to

TH17 CD4 T cells. It will also activate B cells to produce IgA, IgM, and IgG2 for immunity against extracellular bacteria. The cytokine storm during ARDS now explained. It is worth noting that both innate immunity and adaptive immunity including neutrophils and lymphocytes are triggered. Thus, antibody against bacteria as well as autoantibody can be generated. The most common autoantibody found in ARDS is IL-8 autoantibody. IL-8 is the main chemoattractant in pulmonary tissue. It was first identified in lung giant cell lines. The immune-complex of IL-8 and IL-8 autoantibody can further recruit and activate neutrophils. IL-8 autoantibody is also related to the prognosis of ARDS. In other conditions inducing ARDS such as trauma, burn, pancreatitis, or hemorrhagic shock, the presence of autoantibody can cause the sustain of ARDS disease progress. Besides, IL-8 has high affinity to bind to the heparin sulfate and chondroitin sulfate enriched lung tissue. And, IL-8 retention in pulmonary tissue can further recruit neutrophils to lung. It can explain why IL-8 secreted from distant site such as pancreas during acute pancreatitis can cause ARDS.

Bacterial infection is the most common risk factor of ARDS. However, certain pathogens other than bacteria also are risks for developing ARDS. Plasmodium falciparum malarial infection can also cause the complication of ARDS. The reason for this is that Plasmodium falciparum can activate heat shock proteins to trigger TH17 immunity to cause ARDS.(author's paper in press) SARS-CoV and H1N1 Avian flu virus can also down-regulate normal anti-viral interferon-α/β and up-regulate TH17 immunity to trigger ARDS. (author's paper in press: Viral Immunology) Thus, the above phenomonons suggest that TH17 inflammation is the key to the pathogenesis of ARDS. If different pathogens lead to a common pathway of TH17 immunity, they will cause the same consequence of ARDS. It is also seen in burn, trauma, or pancreatitis when TH17 autoimmunity is also activated.

In the second proliferative stage, lymphocytes replace neutrophils and become the dominant population in ARDS. These lymphocytes are TH17 lymphocytes and subsequent Treg lymphocytes. TH17 helper cells can secrete TH17 cytokines such as IL-17, IL-1, IL-6, and TNF-α to continue the inflammatory process. However, once the bacterial antigen during sepsis is cleared. Toll-like receptor signaling is stopped, and no further proinflammatory cytokines such as IL-6 is synthesized. In addition, no further IL-8 is synthesized. IL-8 is the autoantigen for generating IL-8 autoantibody in ARDS. If there is no further IL-8 antoantigen, IL-8 autoantibody producing B cells will stop to proliferate. In TH17 immunity, both TGF-β and IL-6 are two important triggering cytokines. If there is no longer IL-6 signaling, only TGF-β is generated. IL-6

is the key factor to regulate the balance between Treg cells and TH17 cells. If there is enough IL-6, Treg cells will become TH17 cells. If there is not enough IL-6, TGF-β secreting Treg cells will be maintained. Thus, in the third fibrosis stage, TGF-β secreting Treg cells are the dominant effector cells in ARDS. TGF-β is a very strong fibrosis promoting agent. TGF-β will promote the synthesis of multiple collagen genes. Thus, overproduction of TGF-β in lung tissue will cause pulmonary fibrosis. TGF-β caused fibrosis is usually a process for repairing cavity after bacterial infection locus such as abscess. This mechanism can solve many controversial studies before. Several studies found that TLR4 and heat shock proteins can aggravate ARDS. However, another studies found that TLR4 or heat shock protein can protect from pulmonary fibrosis after acute lung injury. It is because TLR and heat shock signaling can maintain the activation of proinflammatory cytokines such as IL-6. Thus, no solely TGF-β overproduction happens for lung fibrosis. Thus, TH17 and Treg inflammatory process can fully explain the pathogenesis of ARDS. After knowing the complete pathophysiology of acute respiratory distress syndrome, we can develop better treatment strategies to managing this highly detrimental disease.

References

Howrylak J.A. et al. Discovery of the gene signature for acute lung injury in patients with sepsis. Physiol Genomics 37,133-139 (2009)

Rotunno M et al. A gene expression signature from peripheral whole blood for stage 1 lung adenocarcinoma. Cancer Prevention Research 4,1599-1608 (2011)

Figure legends

Figure 1. RMA express plot for selecting samples in normal healthy controls.
1-A NUSE boxplot for normal control
1-B RLE boxplot for normal control
1-C RLE-NUSE multiplot for normal control
1-D RLE-NUSE T2 plot for normal control
1-E Raw data Boxpolt for normal control

Figure 2. RMA express plot for selecting samples in ARDS patients.
2-A NUSE boxplot for ARDS patients
2-B RLE boxplot for ARDS patients
2-C RLE-NUSE multiplot for ARDS patients
2-D RLE-NUSE T2 plot for ARDS patients
2-E Raw data Boxplot for ARDS patients

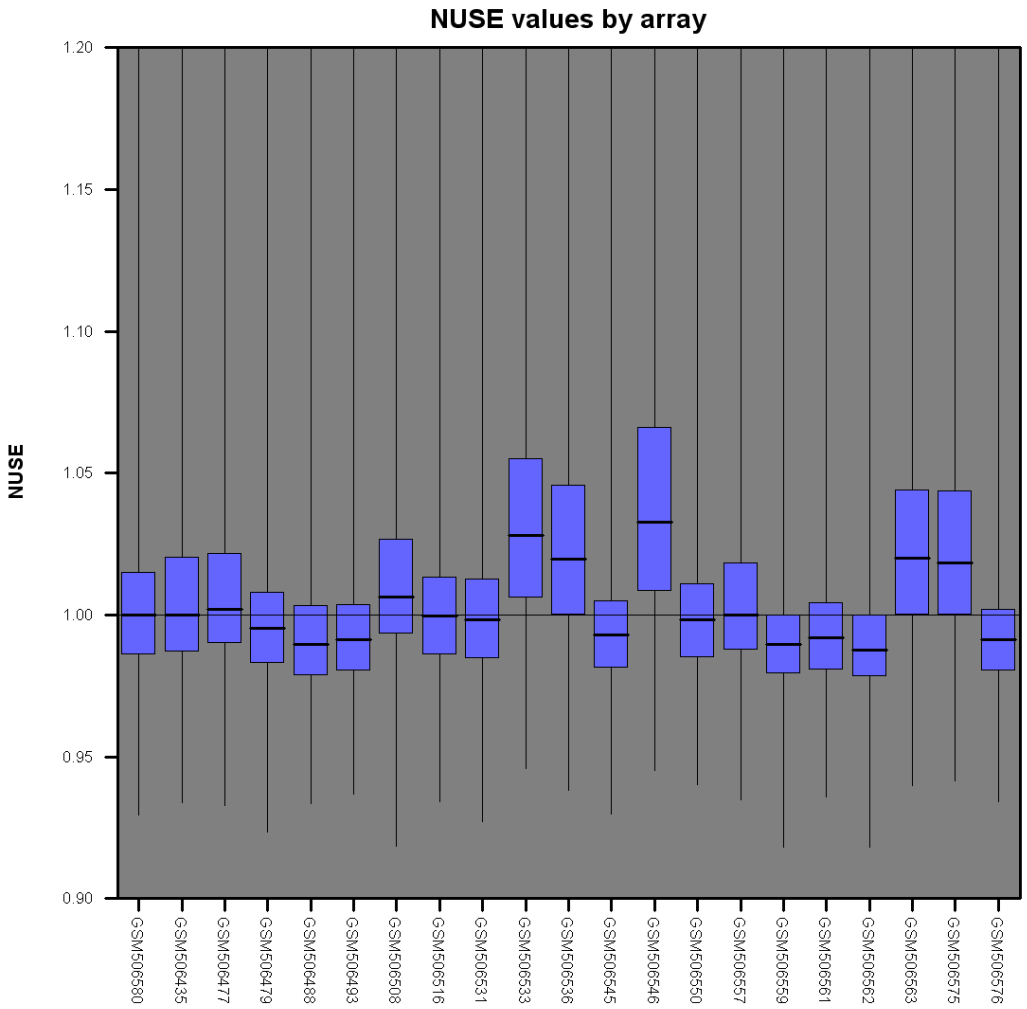
NUSE values by array
NUSE
1.20
1.15
1.10
1.05
1.00
0.95
0.90
GSM506580
GSM506435
GSM506477
GSM506479
GSM506488
GSM506493
GSM506508
GSM506516
GSM506531
GSM506533
GSM506536
GSM506545
GSM506546
GSM506550
GSM506557
GSM506559
GSM506561
GSM506562
GSM506563
GSM506575
GSM506576

Figure 1-A

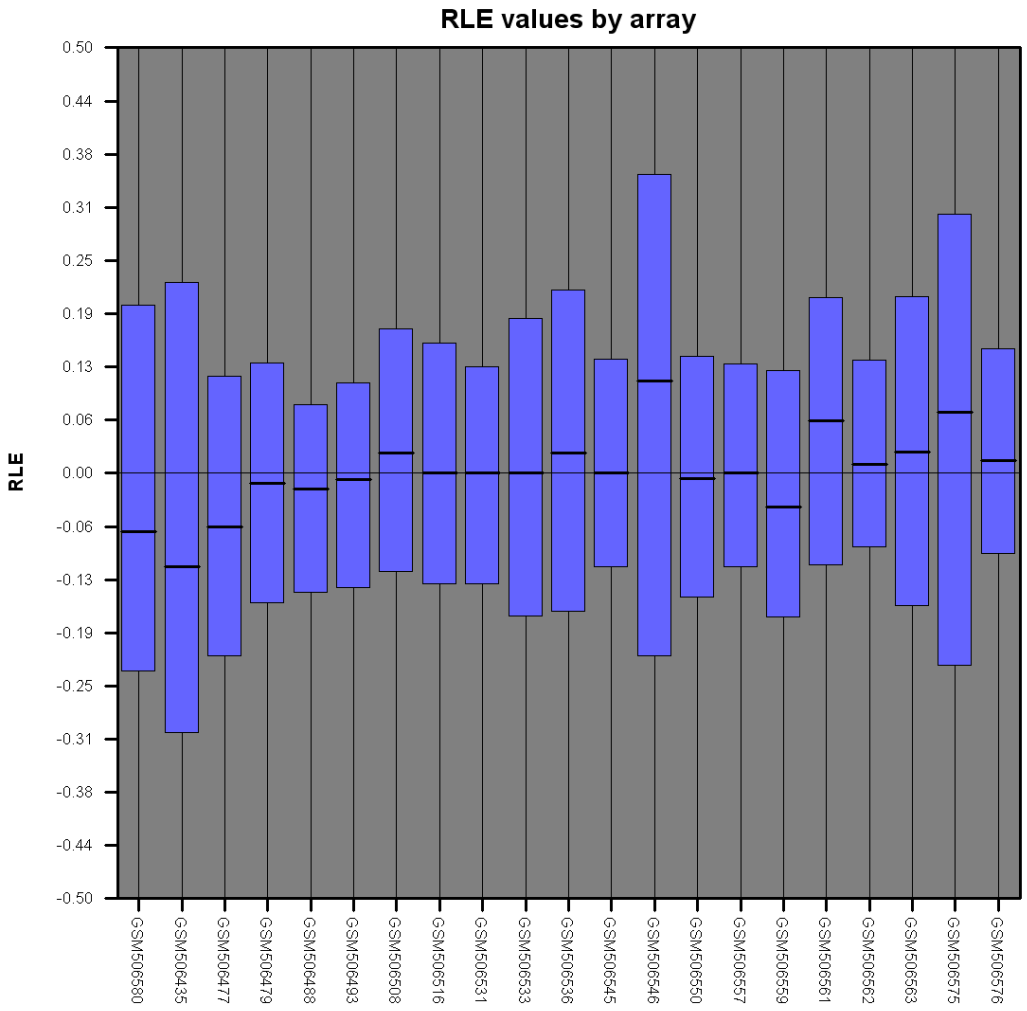
RLE values by array
RLE
0.50
0.44
0.38
0.31
0.25
0.19
0.13
0.06
0.00
-0.06
-0.13
-0.19
-0.25
-0.31
-0.38
-0.44
-0.50
GSM506580
GSM506435
GSM506477
GSM506479
GSM506488
GSM506493
GSM506508
GSM506516
GSM506531
GSM506533
GSM506536
GSM506545
GSM506546
GSM506550
GSM506557
GSM506559
GSM506561
GSM506562
GSM506563
GSM506575
GSM506576

Figure 1-B

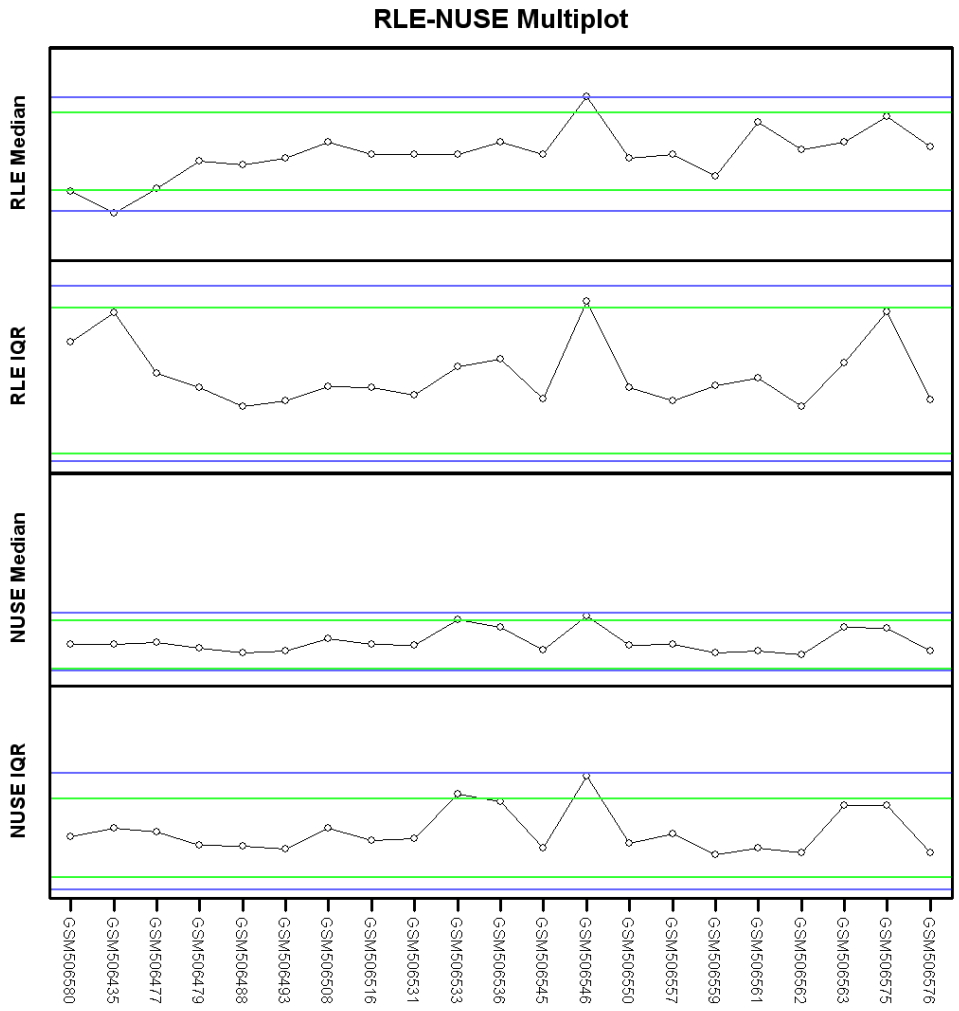
RLE-NUSE Multiplot
RLE Median
RLE IQR
NUSE Median
NUSE IQR
GSM506580
GSM506435
GSM506477
GSM506479
GSM506488
GSM506493
GSM506508
GSM506516
GSM506531
GSM506533
GSM506536
GSM506545
GSM506546
GSM506550
GSM506557
GSM506559
GSM506561
GSM506562
GSM506563
GSM506575
GSM506576

Figure 1-C

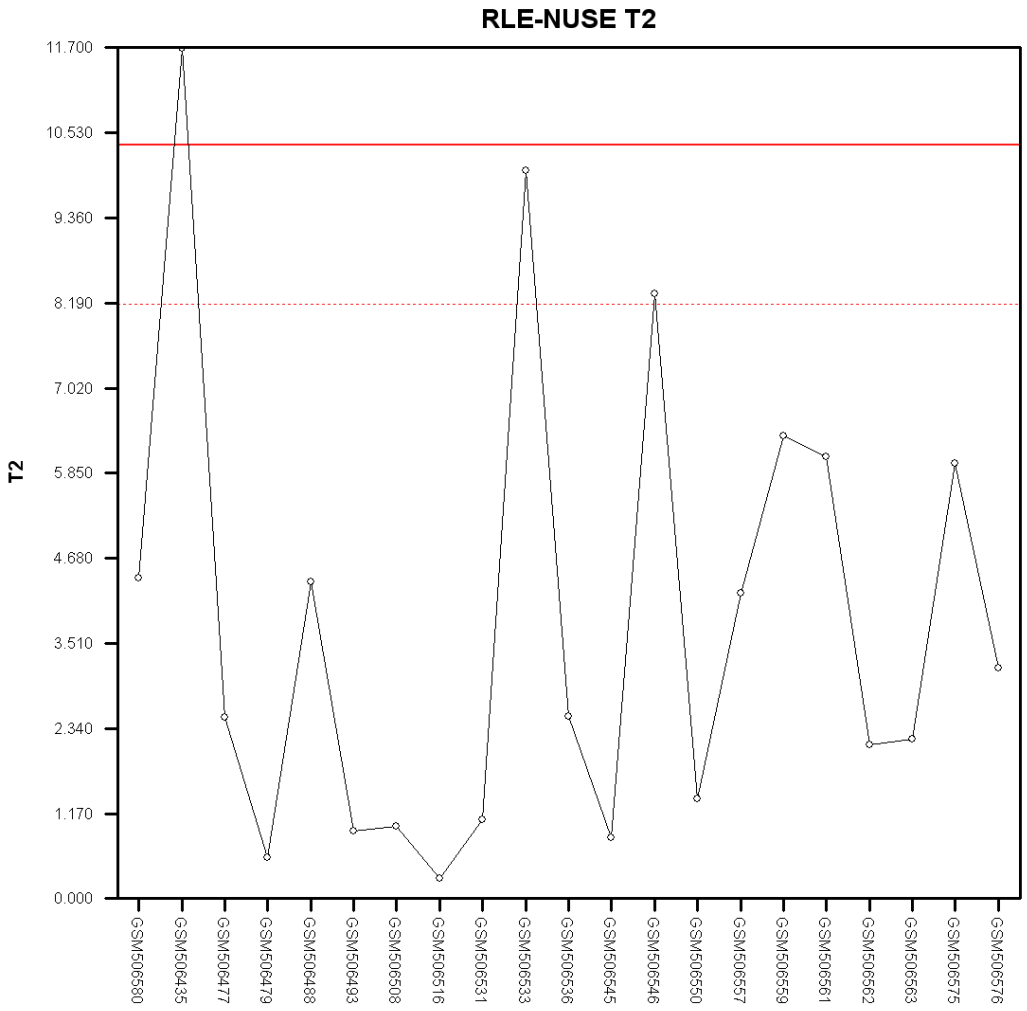
RLE-NUSE T2
T2
11.700
10.530
9.360
8.190
7.020
5.850
4.680
3.510
2.340
1.170
0.000
GSM506580
GSM506435
GSM506477
GSM506479
GSM506488
GSM506493
GSM506508
GSM506516
GSM506531
GSM506533
GSM506536
GSM506545
GSM506546
GSM506550
GSM506557
GSM506559
GSM506561
GSM506562
GSM506563
GSM506575
GSM506576

Figure 1-D

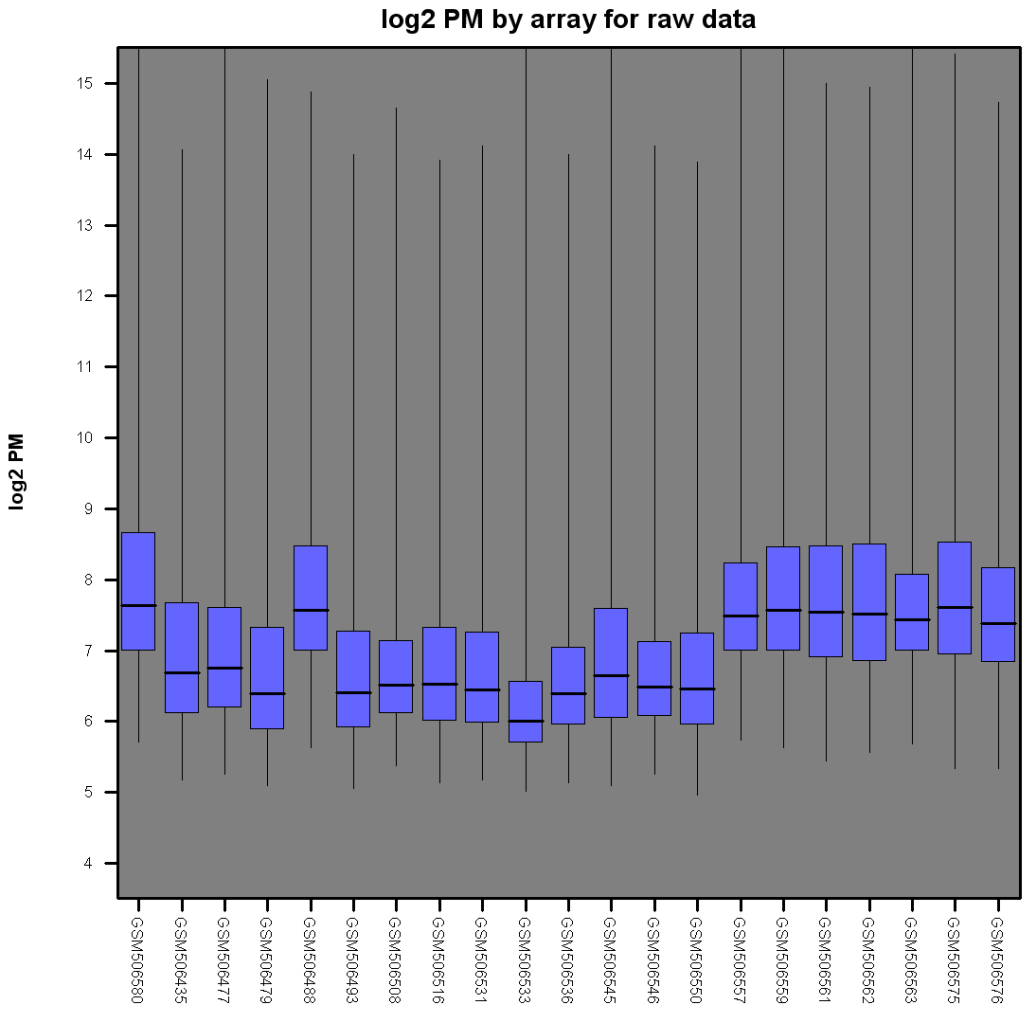
log2 PM by array for raw data
log2 PM
15
14
13
12
11
10
9
8
7
6
5
4
GSM506580
GSM506435
GSM506477
GSM506479
GSM506488
GSM506493
GSM506508
GSM506516
GSM506531
GSM506533
GSM506536
GSM506545
GSM506546
GSM506550
GSM506557
GSM506559
GSM506561
GSM506562
GSM506563
GSM506575
GSM506576

Figure 1-E

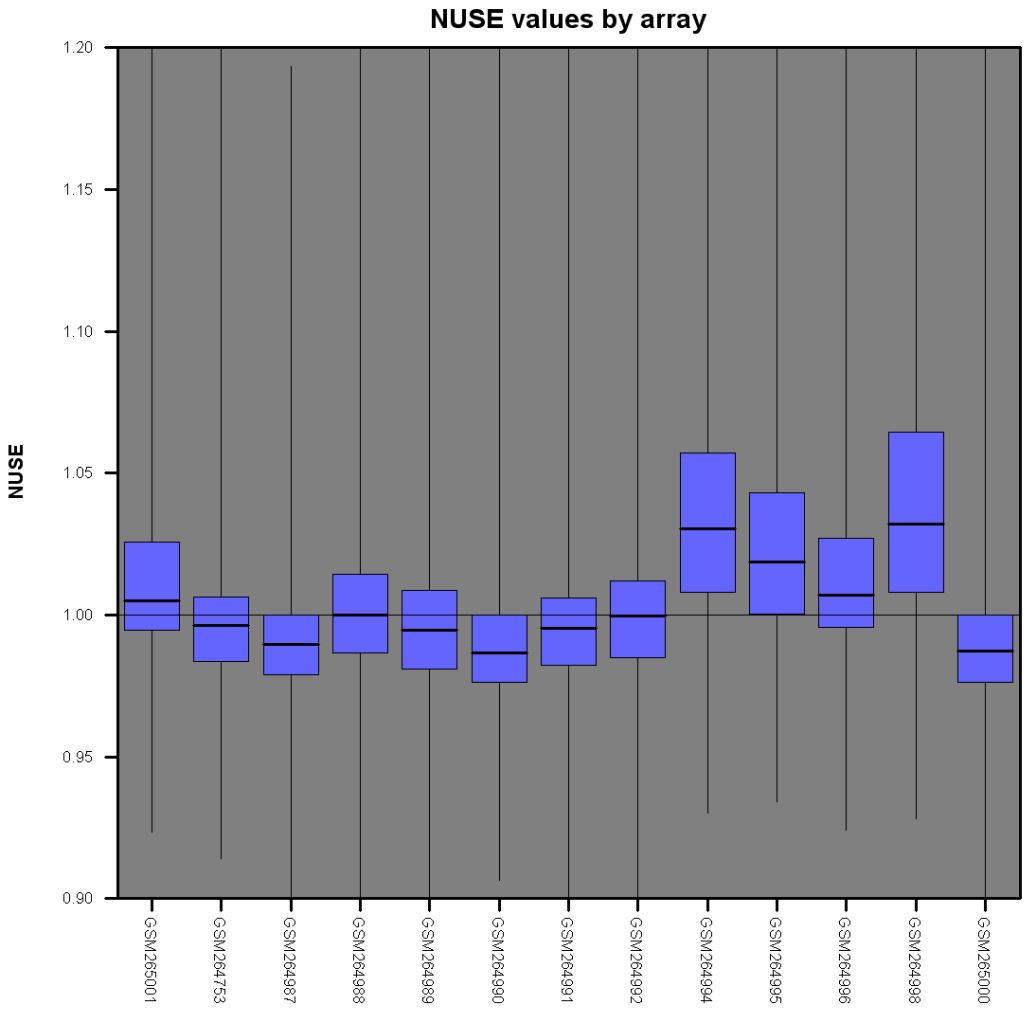
NUSE values by array
NUSE
1.20
1.15
1.10
1.05
1.00
0.95
0.90
GSM265001
GSM264753
GSM264987
GSM264988
GSM264989
GSM264990
GSM264991
GSM264992
GSM264994
GSM264995
GSM264996
GSM264998
GSM265000

Figure 2-A

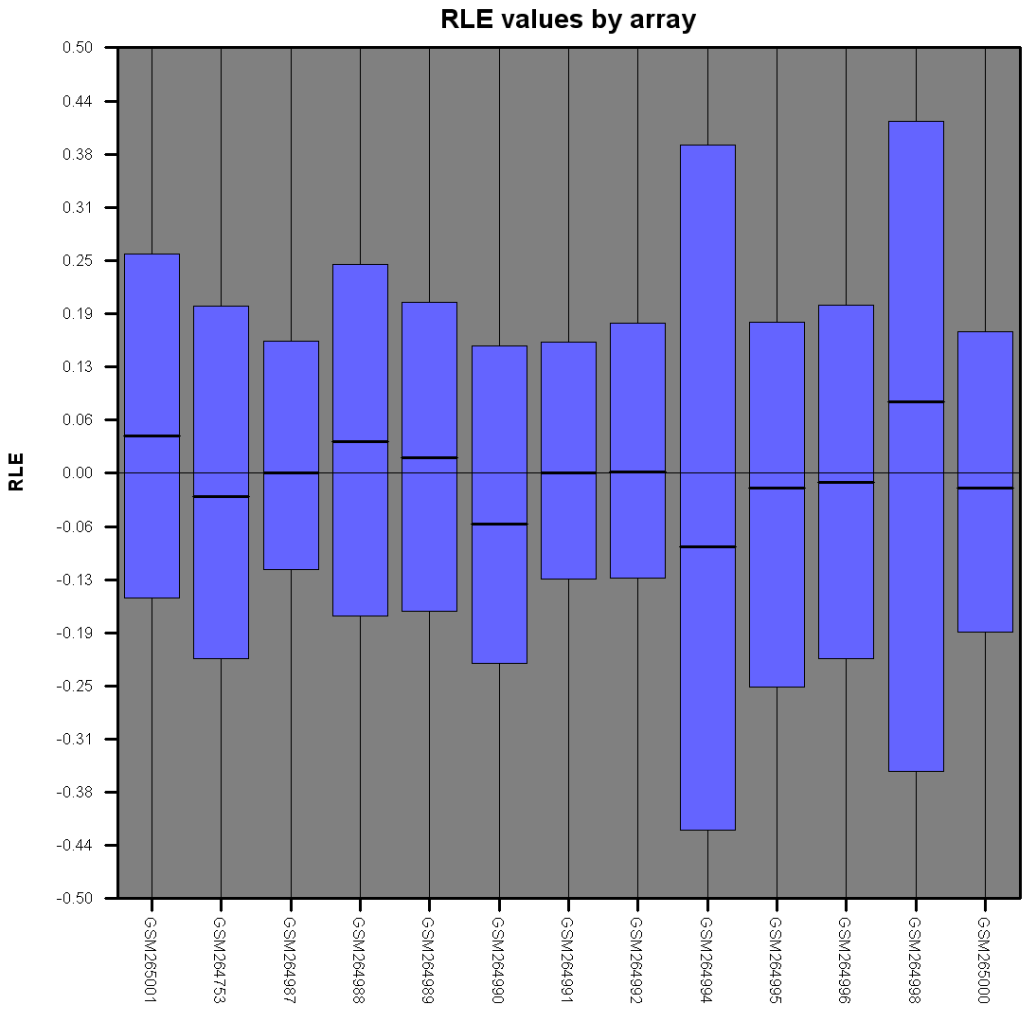
RLE values by array
RLE
0.50
0.44
0.38
0.31
0.25
0.19
0.13
0.06
0.00
-0.06
-0.13
-0.19
-0.25
-0.31
-0.38
-0.44
-0.50
GSM265001
GSM264753
GSM264987
GSM264988
GSM264989
GSM264990
GSM264991
GSM264992
GSM264994
GSM264995
GSM264996
GSM264998
GSM265000

Figure 2-B

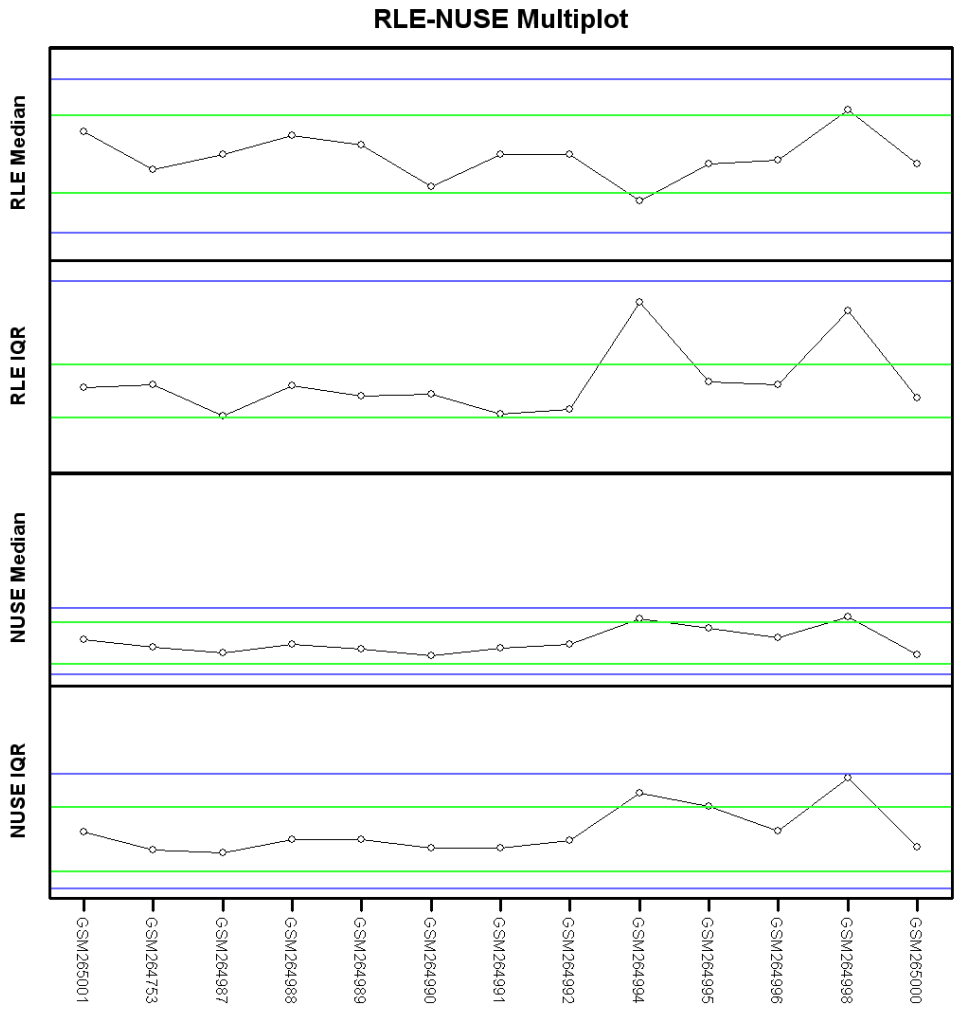
RLE-NUSE Multiplot
RLE Median
RLE IQR
NUSE Median
NUSE IQR
GSM265001
GSM264753
GSM264987
GSM264988
GSM264989
GSM264990
GSM264991
GSM264992
GSM264994
GSM264995
GSM264996
GSM264998
GSM265000

Figure 2-C

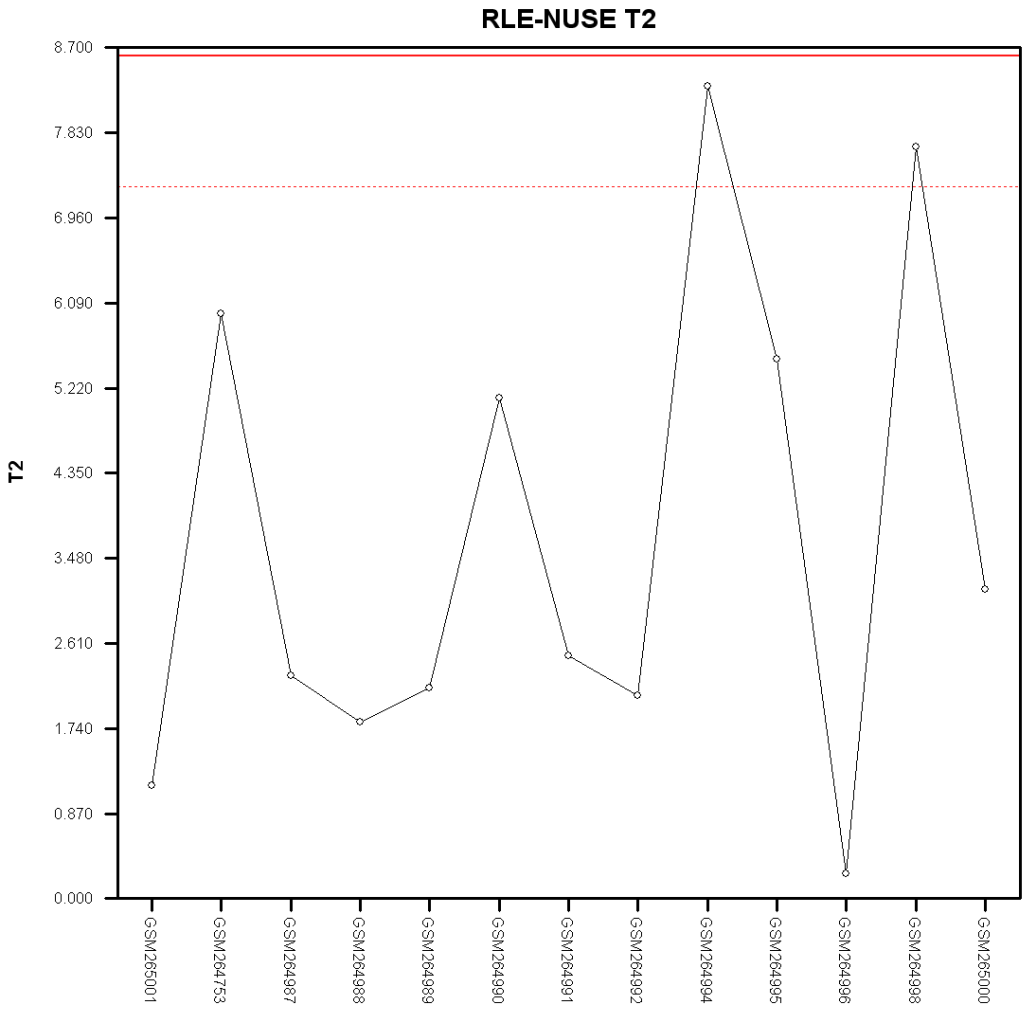
RLE-NUSE T2
T2
8.700
7.830
6.960
6.090
5.220
4.350
3.480
2.610
1.740
0.870
0.000
GSM265001
GSM264753
GSM264987
GSM264988
GSM264989
GSM264990
GSM264991
GSM264992
GSM264994
GSM264995
GSM264996
GSM264998
GSM265000

Figure 2-D

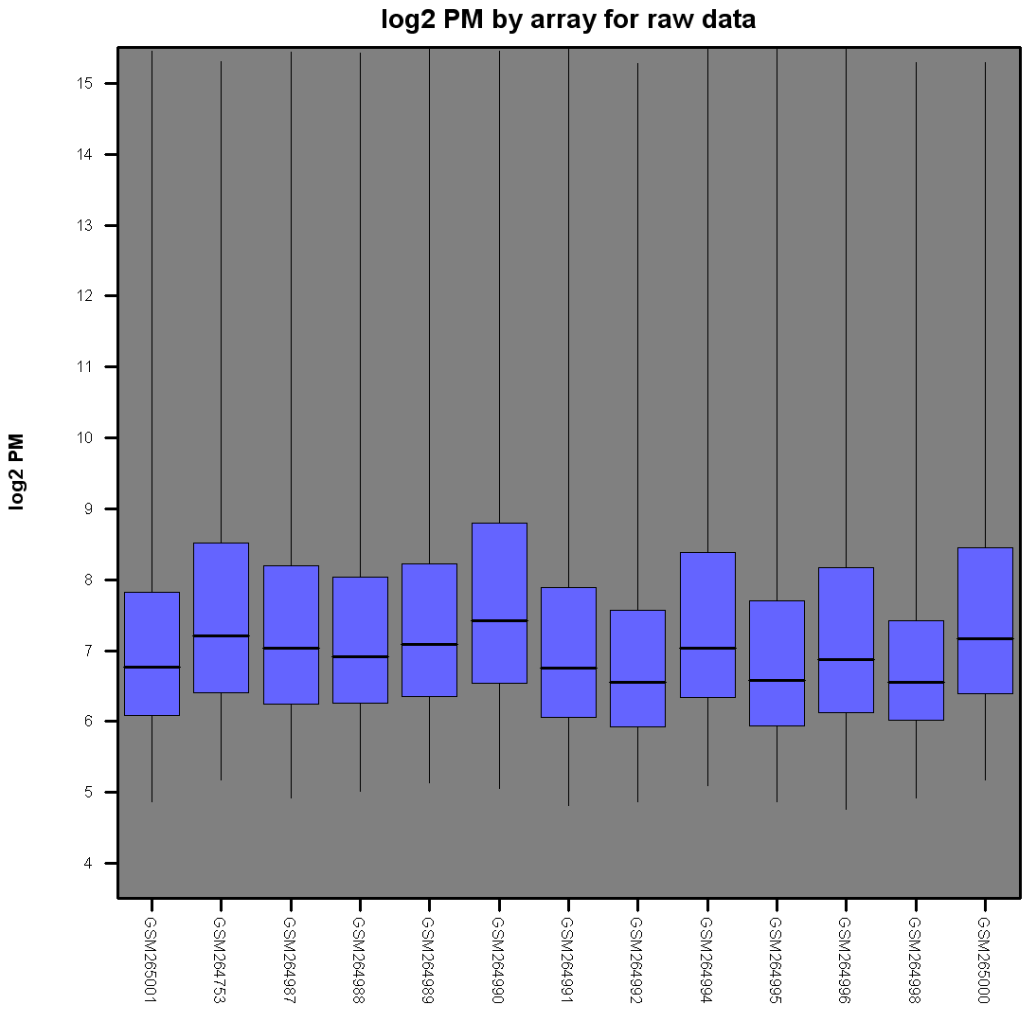
log2 PM by array for raw data
log2 PM
15
14
13
12
11
10
9
8
7
6
5
4
GSM265001
GSM264753
GSM264987
GSM264988
GSM264989
GSM264990
GSM264991
GSM264992
GSM264994
GSM264995
GSM264996
GSM264998
GSM265000

Figure 2-E

Table 1.Toll-likereceptor

Probe Set ID	Pvalue	Arrow	Fold	Gene Symbol
204924_at	6.89E-09	up	3.412607	TLR2
210166_at	1.85E-07	up	2.732714	TLR5
210176_at	3.49E-04	up	2.256822	TLR1
220832_at	1.23E-07	up	5.041227	TLR8
221060_s_at	8.48E-06	up	2.713024	TLR4
219618_at	1.79E-09	up	3.059633	IRAK4
220034_at	3.95E-12	up	7.776434	IRAK3

Table 2.HeatShock Protein

Probe Set ID	Pvalue	Arrow	Fold	Gene Symbol
200598_s_at	5.09E-07	down	2.56764	HSP90B1
200800_s_at	8.10E-08	up	3.152098	HSPA1A /// HSPA1B
202557_at	2.10E-04	up	2.438485	HSPA13
202581_at	1.79E-11	up	6.14778	HSPA1A /// HSPA1B
208744_x_at	1.45E-08	down	2.109862	HSPH1
208815_x_at	6.07E-07	up	2.042983	HSPA4
210338_s_at	4.69E-08	down	2.607109	HSPA8
211969_at	9.22E-14	down	15.02711	HSP90AA1
219284_at	4.74E-04	up	2.277097	HSPBAP1
200941_at	7.08E-09	up	2.341059	HSBP1
200942_s_at	1.40E-05	up	2.092604	HSBP1
				DNAJB6 ///
208810_at	9.82E-04	up	2.226605	TMEM135
209015_s_at	2.14E-07	up	2.790782	DNAJB6
209157_at	9.23E-10	up	3.232302	DNAJA2
212467_at	6.04E-10	up	4.209722	DNAJC13
212908_at	1.42E-10	down	3.075077	DNAJC16
212911_at	3.41E-09	up	3.145019	DNAJC16
202842_s_at	6.90E-04	up	2.138169	DNAJB9
206782_s_at	6.78E-09	up	2.321206	DNAJC4

Table 3.Chemokine

Probe Set ID	Pvalue	Arrow	Fold	Gene Symbol
1405_i_at	5.89E-04	down	2.63913	CCL5
204103_at	8.18E-05	down	2.515743	CCL4
204655_at	7.65E-04	down	2.245439	CCL5
205098_at	2.19E-04	up	2.065441	CCR1
205099_s_at	1.52E-06	down	2.461891	CCR1
205898_at	7.09E-06	down	4.04859	CX3CR1
206337_at	1.20E-07	down	4.466033	CCR7
206366_x_at	5.25E-11	down	5.07455	XCL1
206991_s_at	1.51E-04	down	2.039673	CCR5
208304_at	4.89E-06	down	4.671167	CCR3
				XCL1 ///
214567_s_at	1.62E-08	down	3.339736	XCL2
219161_s_at	4.46E-07	up	2.387246	CKLF
221058_s_at	9.57E-08	up	2.487534	CKLF
200660_at	9.31E-10	up	2.113736	S100A11
200815_s_at	1.43E-11	up	2.871307	PAFAH1B1
202917_s_at	3.16E-09	up	2.744783	S100A8
203535_at	2.25E-13	up	2.882588	S100A9
204351_at	4.60E-04	up	2.44348	S100P
205863_at	7.00E-10	up	4.3815	S100A12

Table4.MHC

Probe Set ID	Pvalue	Arrow	Fold	Gene Symbol
204670_x_at	9.95E-11	down	3.865348	HLA-DRB1/4
208306_x_at	9.05E-09	down	2.986262	HLA-DRB1
208894_at	3.15E-10	down	4.546559	HLA-DRA
209312_x_at	4.77E-09	down	3.655453	HLA-DRB1/4/5
209823_x_at	1.81E-04	down	2.484667	HLA-DQB1
210982_s_at	8.58E-08	down	3.12086	HLA-DRA
211656_x_at	4.91E-05	down	2.002577	HLA-DQB1
211990_at	1.49E-06	down	3.785754	HLA-DPA1
211991_s_at	1.37E-08	down	3.178668	HLA-DPA1
212671_s_at	3.46E-04	down	2.569759	HLA-DQA1/2
212998_x_at	2.28E-05	down	2.456309	HLA-DQB1
213537_at	2.69E-05	down	2.602025	HLA-DPA1
215193_x_at	1.62E-08	down	3.284869	HLA-DRB1/3/4
217478_s_at	1.25E-07	down	2.783175	HLA-DMA
221491_x_at	4.58E-06	down	2.600531	HLA-DRB1/3/4/5
201137_s_at	1.25E-06	down	2.815927	HLA-DPB1
203290_at	4.64E-08	down	5.873323	HLA-DQA1
203932_at	7.50E-07	down	2.382645	HLA-DMB
207565_s_at	2.75E-06	up	2.029287	MR1

Table5.Transcription factor

Probe Set ID	Pvalue	Arrow	Fold	Gene Symbol
205026_at	2.14E-10	up	2.427908	STAT5B
208991_at	5.85E-09	down	3.745264	STAT3
209969_s_at	1.14E-05	down	3.752185	STAT1
212549_at	4.02E-11	up	2.520162	STAT5B
212550_at	3.90E-09	up	2.643262	STAT5B
209189_at	1.67E-04	up	2.499937	FOS
218880_at	4.95E-08	up	3.472536	FOSL2
201473_at	7.18E-08	up	2.59816	JUNB
212501_at	7.61E-09	up	2.240303	CEBPB
213006_at	1.41E-09	up	3.735119	CEBPD
214523_at	2.02E-06	up	2.091157	CEBPE
204039_at	1.40E-08	up	2.398913	CEBPA
204203_at	1.31E-08	up	2.358698	CEBPG
203574_at	1.13E-08	up	4.640286	NFIL3
201502_s_at	5.83E-06	down	2.115988	NFKBIA
205841_at	2.40E-13	up	5.992293	JAK2
205842_s_at	2.73E-06	up	3.288805	JAK2
209604_s_at	4.81E-16	down	6.909352	GATA3
210426_x_at	8.86E-10	down	5.364871	RORA
210479_s_at	9.23E-10	down	6.440884	RORA
210555_s_at	1.03E-05	down	2.547481	NFATC3
210556_at	5.20E-05	down	2.429433	NFATC3
215092_s_at	1.12E-05	down	2.197351	NFAT5
217526_at	3.36E-08	down	3.459827	NFATC2IP
217527_s_at	1.86E-10	down	4.586211	NFATC2IP
217862_at	6.23E-07	down	3.458686	PIAS1
217863_at	1.03E-07	up	2.951054	PIAS1
217864_s_at	1.24E-05	down	2.248191	PIAS1

Table6.Leukotriene & prostaglandin

Probe Set ID	Pvalue	Arrow	Fold	GeneSymbol
208771_s_at	1.53E-08	up	2.726662	LTA4H
210128_s_at	8.83E-10	up	3.067644	LTB4R
216388_s_at	4.30E-09	up	2.518544	LTB4R
215813_s_at	3.33E-05	up	2.706112	PTGS1
215894_at	1.13E-11	down	9.422997	PTGDR
203913_s_at	3.16E-10	up	27.23115	HPGD
203914_x_at	3.10E-09	up	19.87965	HPGD
204445_s_at	1.10E-06	up	2.227303	ALOX5
204446_s_at	3.10E-08	up	2.322821	ALOX5
204614_at	3.94E-06	up	2.905599	SERPINB2
207206_s_at	0.001107	up	2.048875	ALOX12
209533_s_at	1.09E-08	up	2.612623	PLAA
210145_at	1.31E-09	up	3.562516	PLA2G4A
210772_at	3.05E-08	up	4.401296	FPR2
210773_s_at	3.42E-06	up	3.867929	FPR2
213572_s_at	2.12E-12	up	6.133628	SERPINB1
214366_s_at	4.55E-09	up	3.975351	ALOX5

Table7.MMP and FGF

Probe Set ID	Pvalue	Arrow	Fold	Gene Symbol
207329_at	1.17E-08	up	28.02386	MMP8
207890_s_at	1.46E-09	up	3.310085	MMP25
203936_s_at	2.84E-12	up	11.50853	MMP9
205110_s_at	2.26E-06	up	5.236618	FGF13
201666_at	1.46E-08	up	2.519345	TIMP1
203167_at	2.47E-10	up	3.173297	TIMP2
219295_s_at	7.61E-07	up	6.184153	PCOLCE2
219625_s_at	3.39E-16	down	6.705469	COL4A3BP
200827_at	2.27E-07	up	2.158958	PLOD1
200654_at	1.47E-09	up	2.244832	P4HB
201940_at	2.24E-08	up	5.123088	CPD
201941_at	8.36E-08	up	4.763787	CPD
201942_s_at	2.76E-06	up	3.149759	CPD
201943_s_at	6.79E-10	up	6.419939	CPD
202304_at	1.23E-09	up	3.617562	FNDC3A
203044_at	1.34E-05	up	3.342165	CHSY1
203284_s_at	2.64E-08	up	3.515453	HS2ST1
203285_s_at	9.15E-10	up	2.626396	HS2ST1
207165_at	7.94E-05	up	2.063695	HMMR
207543_s_at	9.43E-07	up	2.718742	P4HA1
211945_s_at	0.001738	up	2.065411	ITGB1
218718_at	2.24E-10	up	12.04417	PDGFC
219049_at	1.52E-08	up	7.475137	CSGALNACT1
219403_s_at	1.33E-07	up	5.223431	HPSE
222235_s_at	3.83E-10	up	13.31196	CSGALNACT2

Table8.Complement

Probe Set ID	Pvalue	Arrow	Fold	Gene Symbol
200983_x_at	1.18E-09	up	4.196889	CD59
200984_s_at	1.67E-10	up	4.910066	CD59
200985_s_at	3.02E-11	up	8.311746	CD59
201925_s_at	3.14E-07	up	6.090309	CD55
201926_s_at	4.95E-09	up	4.097339	CD55
202953_at	5.10E-04	up	2.016919	C1QB
205786_s_at	9.34E-11	up	3.896006	ITGAM
206244_at	5.96E-11	up	7.560091	CR1
209906_at	5.21E-09	up	5.687038	C3AR1
210184_at	2.03E-05	up	2.185833	ITGAX
212463_at	3.67E-08	up	3.248518	CD59
217552_x_at	1.83E-09	up	3.938783	CR1
218232_at	2.16E-05	up	3.030927	C1QA
218983_at	2.04E-07	up	3.029844	C1RL
220088_at	2.45E-06	up	2.500003	C5AR1
205033_s_at	7.03E-06	up	6.365769	DEFA1/1B/3
207269_at	1.49E-04	up	6.195451	DEFA4

Table9.Cathepsin

Probe Set ID	Pvalue	Arrow	Fold	Gene Symbol
202450_s_at	4.73E-06	up	2.020977	CTSK
203758_at	3.84E-07	down	2.476479	CTSO
205653_at	4.28E-04	up	3.634934	CTSG
210042_s_at	5.41E-05	up	2.824491	CTSZ
214450_at	9.49E-04	down	2.150796	CTSW
200661_at	1.10E-07	up	2.603046	CTSA
200766_at	3.02E-11	up	3.793397	CTSD
201487_at	2.22E-07	up	3.024736	CTSC
203948_s_at	6.35E-04	up	2.112642	MPO
203949_at	5.14E-06	up	4.61238	MPO

Table10.CSF

Probe Set ID	Pvalue	Arrow	Fold	Gene Symbol
205159_at	7.47E-05	up	2.272558	CSF2RB
210340_s_at	6.06E-10	up	2.727757	CSF2RA
203591_s_at	4.27E-06	up	2.365631	CSF3R

Table11.Fc receptor

Probe Set ID	Pvalue	Arrow	Fold	Gene Symbol
203561_at	5.57E-08	up	2.06512	FCGR2A
204232_at	6.41E-10	up	2.89912	FCER1G
207674_at	4.21E-07	up	6.511793	FCAR
210992_x_at	2.25E-05	up	2.003132	FCGR2C
211307_s_at	3.73E-07	up	4.462972	FCAR
211734_s_at	7.11E-05	down	4.276542	FCER1A
211816_x_at	2.46E-05	up	2.47651	FCAR
214511_x_at	1.06E-05	up	3.171251	FCGR1B
216950_s_at	4.67E-08	up	5.148257	FCGR1A/1C

Table12.Cytokine & receptor

Probe Set ID	Pvalue	Arrow	Fold	Gene Symbol
203828_s_at	6.11E-04	down	2.216758	IL32
205227_at	4.73E-04	up	2.365252	IL1RAP
205291_at	2.41E-06	down	3.160494	IL2RB
205403_at	5.96E-11	up	9.990063	IL1R2
205707_at	5.70E-06	down	2.016105	IL17RA
205798_at	2.19E-21	down	28.62358	IL7R
205926_at	2.78E-10	down	2.211585	IL27RA
205945_at	9.53E-14	down	13.61186	IL6R
205992_s_at	3.86E-06	up	3.345045	IL15
206618_at	1.05E-11	up	17.52686	IL18R1
207072_at	3.95E-11	up	6.322352	IL18RAP
208200_at	3.63E-09	down	4.584162	IL1A
208930_s_at	7.16E-10	down	4.59278	ILF3
211367_s_at	5.56E-05	up	2.343338	CASP1
211368_s_at	1.99E-04	up	2.023957	CASP1
211372_s_at	2.35E-10	up	17.05508	IL1R2
212195_at	9.18E-05	up	2.753398	IL6ST
212196_at	1.44E-05	up	2.060642	IL6ST
212657_s_at	3.37E-06	up	2.343125	IL1RN
217489_s_at	9.59E-13	down	3.415206	IL6R
202948_at	1.06E-10	up	9.925212	IL1R1
203233_at	1.18E-09	up	3.541053	IL4R
205016_at	6.86E-09	up	4.867131	TGFA
201506_at	1.41E-04	down	2.289291	TGFBI
203085_s_at	1.35E-05	up	2.13325	TGFB1
204731_at	3.89E-15	down	10.80744	TGFBR3
206026_s_at	7.23E-06	up	4.685213	TNFAIP6
206222_at	3.55E-07	down	2.189329	TNFRSF10C
207536_s_at	4.78E-06	down	2.923358	TNFRSF9
207643_s_at	1.78E-08	up	2.618468	TNFRSF1A
207907_at	3.57E-08	down	3.31319	TNFSF14
208296_x_at	8.56E-05	up	2.646926	TNFAIP8
210260_s_at	5.80E-05	up	2.88896	TNFAIP8
214329_x_at	2.56E-04	up	2.679365	TNFSF10
202509_s_at	8.86E-10	down	2.258532	TNFAIP2
206332_s_at	3.11E-05	up	2.16889	IFI16

208114_s_at	6.33E-16	down	6.286403	ISG20L2
208965_s_at	1.52E-08	down	6.302218	IFI16
211676_s_at	1.42E-07	up	4.556334	IFNGR1
220577_at	8.19E-07	down	2.331832	GVINP1
201642_at	8.60E-08	up	2.225393	IFNGR2
202269_x_at	1.73E-05	down	4.987527	GBP1
202727_s_at	9.68E-08	up	3.452631	IFNGR1
204191_at	2.33E-07	up	2.031339	IFNAR1
204415_at	0.004538	up	2.774495	IFI6
204439_at	0.004491	down	3.991523	IFI44L
204747_at	5.65E-04	down	3.737294	IFIT3
204786_s_at	5.62E-17	down	6.491528	IFNAR2
200704_at	1.66E-07	up	2.056096	LITAF
201108_s_at	3.76E-05	up	2.314963	THBS1
201109_s_at	2.60E-05	up	3.128824	THBS1
201110_s_at	1.47E-08	up	7.142229	THBS1
204780_s_at	3.86E-04	up	2.720255	FAS
204781_s_at	9.11E-05	up	2.032212	FAS
204961_s_at	5.23E-06	up	2.092114	NCF1B1C
207677_s_at	5.21E-09	up	3.07743	NCF4
221601_s_at	1.46E-09	down	4.684259	FAIM3
221602_s_at	2.90E-10	down	3.944784	FAIM3

Table13.CD molecules

Probe Set ID	Pvalue	Arrow	Fold	Gene Symbol
200663_at	1.23E-10	up	2.64625	CD63
201005_at	1.19E-06	up	4.053223	CD9
202878_s_at	1.20E-04	up	2.316249	CD93
202910_s_at	1.39E-04	up	2.078598	CD97
203645_s_at	1.60E-06	up	7.818829	CD163
203799_at	0.002884	up	2.038077	CD302
204489_s_at	3.25E-10	up	2.475646	CD44
204490_s_at	1.31E-08	up	2.582747	CD44
204627_s_at	3.45E-05	up	3.667203	ITGB3
204661_at	7.10E-06	down	2.483425	CD52
205173_x_at	7.28E-08	up	4.151193	CD58
205758_at	1.12E-04	down	3.211919	CD8A
205789_at	4.22E-05	up	2.844588	CD1D
205831_at	2.21E-07	down	4.421892	CD2
205987_at	1.13E-07	down	2.078875	CD1C
205988_at	1.13E-15	down	5.71907	CD84
206150_at	2.30E-08	down	2.506513	CD27
206488_s_at	6.10E-04	up	2.481129	CD36
206493_at	5.05E-06	up	3.000028	ITGA2B
206494_s_at	7.02E-04	up	3.137038	ITGA2B
206761_at	3.30E-04	down	2.113857	CD96
206804_at	6.16E-10	down	4.490583	CD3G
208405_s_at	8.52E-05	up	2.330166	CD164
208650_s_at	7.09E-07	up	6.548884	CD24
208651_x_at	6.39E-08	up	4.732706	CD24
208652_at	1.21E-07	up	2.66052	PPP2CA
208653_s_at	6.26E-10	up	5.120652	CD164
208654_s_at	3.97E-06	up	5.608513	CD164
209555_s_at	2.95E-04	up	2.950439	CD36
209771_x_at	1.32E-07	up	6.559978	CD24
209835_x_at	1.06E-06	up	2.202673	CD44
210031_at	1.34E-06	down	3.413696	CD247
210184_at	2.03E-05	up	2.185833	ITGAX
210895_s_at	2.39E-04	down	2.251445	CD86
211744_s_at	5.92E-08	up	4.172478	CD58
211893_x_at	8.92E-10	down	2.082775	CD6

211900_x_at	5.14E-12	down	2.56049	CD6
212014_x_at	7.54E-07	up	2.308336	CD44
212063_at	4.06E-06	up	2.119029	CD44
213958_at	1.17E-06	down	2.205519	CD6
215049_x_at	2.45E-06	up	7.967604	CD163
215240_at	1.19E-08	up	2.467146	ITGB3
216233_at	4.99E-06	up	6.556412	CD163
216331_at	0.001993	up	2.434621	ITGA7
216379_x_at	5.86E-08	up	7.598393	CD24
216942_s_at	1.49E-05	up	3.193467	CD58
216956_s_at	1.65E-04	up	2.29709	ITGA2B
217523_at	9.19E-10	down	6.259623	CD44
219669_at	4.80E-13	up	52.83338	CD177
222061_at	2.36E-09	up	3.870316	CD58
266_s_at	6.15E-09	up	9.687818	CD24

Table14.NK/CTL molecules

Probe Set ID	Pvalue	Arrow	Fold	Gene Symbol
205821_at	8.68E-07	down	3.717665	KLRK1
206666_at	6.47E-06	down	3.898898	GZMK
207460_at	5.21E-06	down	2.196101	GZMM
207795_s_at	8.11E-05	down	2.646551	KLRD1
210164_at	3.84E-06	down	4.671744	GZMB
210288_at	2.27E-09	down	5.673069	KLRG1
210321_at	2.14E-05	down	6.098404	GZMH
210606_x_at	2.18E-05	down	2.995347	KLRD1
210915_x_at	2.72E-06	down	3.166231	TRBC1
210972_x_at	3.84E-07	down	3.223779	TRAC/J17/V20
211796_s_at	2.86E-06	down	3.233982	TRBC1/C2
211902_x_at	3.75E-06	down	2.651879	TRD@
213193_x_at	8.35E-07	down	3.394675	TRBC1
213539_at	1.57E-06	down	3.240318	CD3D
213830_at	1.16E-08	down	3.694018	TRD@
214470_at	4.30E-04	down	2.832583	KLRB1
214617_at	2.56E-04	down	3.489038	PRF1
215338_s_at	2.44E-19	down	13.36511	NKTR
215806_x_at	2.27E-05	down	3.907998	TARP/TRGC2
216191_s_at	3.85E-06	down	5.215065	TRDV3
216920_s_at	1.31E-06	down	5.017736	TARP/TRGC2
217143_s_at	6.84E-08	down	6.090665	TRD@
220646_s_at	0.004097	down	2.571194	KLRF1
37145_at	4.61E-06	down	5.027259	GNLY